

Facile Extraction and Characterization of Calcium Hydroxide From Paper Mill Waste Sludge of Bangladesh

Mohammad Robel Molla

Bangladesh Council of Scientific and Industrial Research

Most. Hosney Ara Begum

Bangladesh Council of Scientific and Industrial Research

Syed Farid Uddin Farhad (✉ sf1878@my.bristol.ac.uk)

Bangladesh Council of Scientific and Industrial Research <https://orcid.org/0000-0002-0618-8679>

A. S. M. Asadur Rahman

Bangladesh Council of Scientific and Industrial Research

Nazmul Islam Tanvir

Bangladesh Council of Scientific and Industrial Research

Muhammad Shahriar Bashar

Bangladesh Council of Scientific and Industrial Research

Riyadh Hossen Bhuiyan

Bangladesh Council of Scientific and Industrial Research

Md. Sha Alam

Bangladesh Council of Scientific and Industrial Research

Mohammad Sajjad Hossain

Bangladesh Council of Scientific and Industrial Research

Mir Tamzid Rahman

Bangladesh Council of Scientific and Industrial Research

Research Article

Keywords: Paper mill sludge (PMS), Calcium hydroxide, FTIR, XRD, SEM, Wavelength dispersive X-ray Fluorescence, Raman spectroscopy

Posted Date: November 11th, 2021

DOI: <https://doi.org/10.21203/rs.3.rs-1052997/v1>

License:  This work is licensed under a Creative Commons Attribution 4.0 International License.

[Read Full License](#)

Facile extraction and Characterization of Calcium Hydroxide from Paper Mill Waste Sludge of Bangladesh

Mohammad Robel Molla^{1,‡}, Most. Hosney Ara Begum^{1,‡*}, Syed Farid Uddin Farhad^{1,*}, A. S. M. Asadur Rahman², Nazmul Islam Tanvir¹, Muhammad Shahriar Bashar³, Riyadh Hossen Bhuiyan⁴, Md. Sha Alam⁵, Mohammad Sajjad Hossain¹, and Mir Tamzid Rahman⁶

[‡] *Contributed equally to this work.*

¹*BCSIR Laboratories, Dhaka, Bangladesh Council of Scientific and Industrial Research, Dhaka-1205 Bangladesh*

²*Department of Chemistry, Comilla University, Cumilla-3506*

³*Institute of Fuel Research and Development, Bangladesh Council of Scientific and Industrial Research, Dhaka-1205 Bangladesh*

⁴*Fiber and Polymer Research Division, Bangladesh Council of Scientific and Industrial Research, Dhaka-1205 Bangladesh*

⁵*Institute of Mining, Mineralogy & Metallurgy, Bangladesh Council of Scientific and Industrial Research, Joypurhat-5900, Bangladesh*

⁶*Department of Chemistry, Jahangirnagar University, Savar, Dhaka-1342, Bangladesh*

**Correspondence address:*

Dr. Most. Hosney Ara Begum, CSO
& Dr. Syed Farid Uddin Farhad, PSO

Industrial Physics Division,

BCSIR Laboratories, Dhaka, BCSIR, Dhaka-1205

Email: hosneyara@gmail.com ; s.f.u.farhad@bcsir.gov.bd

Abstract

Herein, paper mill waste sludge (PMS) from two different sources has been investigated to extract calcium hydroxide, $\text{Ca}(\text{OH})_2$ by a facile and inexpensive extraction process. This green process exploits typical chemical precipitation (CP) in an aqueous medium at room temperature to develop an economically and industrially viable technique for the effective utilization of calcium-containing waste sludge. PMS samples, collected from local paper mill plants of Bangladesh, were the main precursors wherein HCl and NaOH were utilized for chemical treatment. The as-synthesized products were analyzed by a variety of characterization tools including X-ray diffraction (XRD), Fourier transform infrared (FTIR) spectroscopy, Raman spectroscopy, Scanning electron microscopy (SEM), and Energy Dispersive X-ray (EDX) elemental analyses. Our studies confirm that the extracted product contains $\text{Ca}(\text{OH})_2$ as a major content, albeit it also includes CaCO_3 phase formed owing to the inescapable carbonation process from the surrounding environment. The particle size of the synthesized products is in the range of 450 - 500 nm estimated from SEM micrographs. The crystallite domain size of the same estimated from XRD analyses and was found to be ~47 nm and ~31 nm respectively for product-A and product-B considering major (101) Bragg peak of $\text{Ca}(\text{OH})_2$. The yield percentage of the isolated products is about 65% for samples collected from both sources.

Keywords: Paper mill sludge (PMS), Calcium hydroxide, FTIR, XRD, SEM, Wavelength dispersive X-ray Fluorescence, Raman spectroscopy

1. Introduction

Pulp and paper industries are generating a vast amount of pulp per year all around the world to fulfil the ever-growing demand of papers and packaging materials for diverse applications [1-4]. A suitable estimation reported that the production volume of paper and cardboard in developed countries were approximately 1,000 metric tons in 2019 [5]. In 2017, the amount of global production of paper and cardboard reached approximately 419.7 million metric tons which were approximately 391.2 – 410.9 million metric tons from 2008 to 2016 [6]. During the production of paper and pulp processing, a huge amount of calcium carbonate (CaCO_3) is utilized. Consequently, a large volume of paper mill sludge (PMS) has been generated worldwide which contains an enormous amount of CaCO_3 . In many countries, except some well-renowned industries, a large number of pulp and paper industries are disposing this PMS without further utilizing/ recycling/ extracting calcium compounds, causing various types of ecological and environmental negative impacts. Therefore, it is a pressing necessity to utilizing this PMS for value added-products as well as to address its negative impacts on our environment. On the other hand, calcium hydroxide ($\text{Ca}(\text{OH})_2$) materials have variety of applications such as advanced bone repairing [7], de-acidification and wood conversion [8], protection of cultural heritage [9], Calcium oxide (CaO) synthesis from $\text{Ca}(\text{OH})_2$ [10, 11], using as a binding agent in the production of Portland cement [12, 13], advanced application in the biomedical research [14], removal of phosphorus from aqueous medium [1], direct and indirect pulp processing [15], dental research [16] and so forth.

Numerous methods have been developed for the synthesis of calcium hydroxide such as precipitation [17], sol-gel-method [18], water-in-oil micro-emulsions [19], sono-chemical [20] and hydrogen plasma-mental reaction [21]. According to literature studied, $\text{Ca}(\text{OH})_2$ were synthesized by chemical precipitation (CP) process by different researchers [22-31] where salts of calcium chloride or nitrates and sodium hydroxide were the primary starting materials. Various types of waste materials were also used as calcium sources such as snail shell [32], eggshell [33], clamshell [34] and so on. Water-in-Oil process [19], wet chemical process [35], heterogeneous phase synthesis [24], and moisture effect process [34] were also conducted by others. In case of choosing synthesis medium, mainly three types of mediums were utilized such as aqueous [19, 22, 23, 29, 30, 33], organic [19, 24, 25, 27, 28, 31, 35], organic + aqueous [25, 26]. Depending on reaction

conditions, maintaining different temperatures above 90°C were noticed. From the literature cited above, it is also seen that synthesis of Ca(OH)₂ by using CaCl₂/Ca(NO₃)₂/waste materials and NaOH through various typical methods have been performed, however, utilizing waste PMS for synthesizing Ca(OH)₂ have rarely been reported. Our objective of the present study is to extract Ca(OH)₂ from PMS waste material and develop a facile and inexpensive process by chemical treatment or precipitation process at room temperature without utilizing any ionic/non-ionic surfactant in aqueous medium. Because surfactant molecules have the propensity to stick on the surface of particles and the size as well as shape of particles may be affected by the concentration of surfactants and chemical nature [22, 25, 34]. Therefore, the main novelty of this study is the demonstration of a feasible method of Ca(OH)₂ synthesis which has the potential for large-scale production. To that end, the experimental results are presented and discussed below.

2. Materials and methods

Paper mill sludge (PMS) samples were collected from two different local paper mill plants of Bangladesh as calcium containing source materials. First of all, the collected PMS was mixed with distilled water to prepare a homogeneous mixture which was then filtered by a suction pump. After filtration, the mixture was dried in an electric oven at 60 – 65 °C for 2 h in air until complete removal of water. Then it was crashed manually by using a ceramic mortar/pastel. Afterwards, a certain amount of dry-solid sludge was taken in a beaker, mixed with distilled water, and then stirred for 45 min. Then 1.0 M HCl (37%, K46915817529, Merck Germany) was added in solution to dissolve all the calcium contents in the aqueous medium, where pH of the sludge solution was maintained in the range of 2.25 - 2.50. After filtering the acidic solution, the filtrate part (very clear) was taken under base treatment by NaOH (CAS: 1310-73-2, DAEJUNG, Korea, Purity ~98.0%) with maintain a pH above 13.0 and the product formation/precipitation was seen to start within few minutes. The raw and synthesized samples were safely stored into the sample vials for various characterizations (A representative photograph of these samples is shown in [Figure S1](#)).

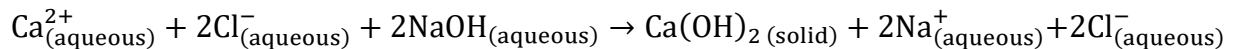
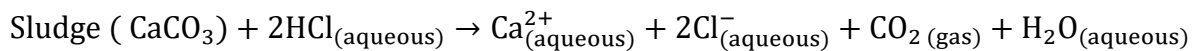
In order to find the characteristic functional groups in the as-synthesis products, the IR spectrum of the samples were recorded in the range of 450 – 4000 cm⁻¹. An FTIR spectrometer with a resolution of 4 cm⁻¹ (Frontier, Perkin-Elmer, UK; Software version 10.4.4.) and the typical

potassium bromide (KBr) pellet technique was utilized for the same. The study of crystal structure along with mineral phase's identification of samples were conducted by means of X-ray diffraction (EMMA GBC Corporation Company) using Cu $K_{\alpha 1}$ (wavelength, $\lambda = 1.54056\text{\AA}$) source operated at 40kV and 30 mA. The X-ray diffraction (XRD) data were recorded in the range of $(2\theta) = 10^\circ - 80^\circ$ with a step size of 0.05° . Raman spectroscopic measurements were performed at room temperature by a Horiba MacroRAM equipment using 780 nm diode laser as excitation (Laser power < 5mW) source. A silicon wafer sample (Raman peak $\sim 520.7\text{ cm}^{-1}$) was used to calibrate spectrometer prior to the data acquisition of the samples. The surface morphology and elemental composition of samples were conducted by a scanning electron microscope (SEM, Zeiss, EVO-18) coupled with an energy dispersive X-ray (EDX) spectrometer (EDX, AMETEK). Prior to synthesis of $\text{Ca}(\text{OH})_2$, the as-collected raw PMSs were characterized by a wavelength dispersive X-ray Fluorescence (WD-XRF) equipment (Rigaku ZSX Primus) to investigate the inorganic contents in the samples.

3. Results and Discussion

3.1. Synthesis

We have examined various batches of PMS samples for acid-base pH optimization and all the necessary information are listed in [Table 1](#). At the beginning of the treatment, the pH value in both acidic and basic medium was not suitable and the amount of the yield was very low. When pH was kept between 2.25 and 2.50 (in acidic medium) and pH value above 13.0 (in basic medium) [1, 15, 23, 31], the amount of product was higher (see [Table 2](#)). In this work our optimized pH values during chemical treatment of sludge were 2.25 – 2.50 (in acidic medium) and above 13.0 (in basic medium). The $\text{Ca}(\text{OH})_2$ formation by the chemical precipitation route involves the following chemical reactions:



In the first batch, the molar concentration of HCl and NaOH was 0.5 M which was considered for examining the effects of different concentrations (HCl and NaOH) on the amount of product formation (Table 1). Finally, 1.0 M concentration of HCl and 3.0 M concentration of NaOH were chosen. The variation of volume of water shown in Table 1 was only to minimize the amount of water used during sample preparation. Sodium hydroxide (NaOH) was used as a precipitator. During insertion of NaOH solution, continuous stirring at a rate of 1300 rpm at room temperature was maintained. After complete precipitation, the product was filtered by a Whatman 40 (GE Healthcare UK Limited, Little Chalfont, and Buckinghamshire, UK) paper. For removal of NaCl, the product was washed several times with deionized water, after which it was dried in an electric oven at 65°C – 70°C for 3 h and preserved in airtight sample bottles. The residual part obtained from acid solution filtration was collected, dried and kept for further research work (e.g., activated carbon).

At optimized P^H value (2.25 – 2.50, in acid and above 13.0, in base) five batches of acid and base treatment for calcium hydroxide isolation were performed for sample (a) and sample (b) (Table S1). The batch numbers were denoted as S-a A, S-a B, S-a C, S-a D and S-a E for sample (a) and S-b A, S-b B, S-b C, S-b D, and S-b E for sample (b). For each sample, a different amount of raw sludge was taken (2.0g, 4.0g, 6.0g, 8.0g, and 10.0g) for all batches A, B, C, D, and E respectively. The amount of water was not fixed and our attempt was to minimize or lower usage of water. For the sample (a) of the first batch, the amount of product was 0.07 g which was found to be greater than that of the sample (b). However, for other batches the amount of product for sample (b) was higher than the sample (a) (Table S1).

Table 1: Optimization of pH value to have the highest product during acid and base treatment of dried raw PMS

<i>Acid and Base treatment of dry sludge for pH adjustment</i>								
Batch No.	Weight of taken sample (g)	The volume of water added in the sample	HCl ml/ M	pH (in HCl)	NaOH ml/ M	pH (in NaOH)	Weight of Product, Ca(OH) ₂ (g)	Weight of Pulp Residue (g)
1	2.0	300	205/0.5	2.87	234/0.5	12.18	0.1000	0.1700
2	2.0	250	55/1.0	2.52	99/1.0	12.64	0.2295	0.2701
3	2.0	250	40/1.0	2.28	200/1.0	13.03	1.0615	0.2614
4	2.0	200	42/1.0	2.10	100/2.0	13.09	1.0462	0.2500
5	2.0	200	50/1.0	1.90	125/2.0	13.05	1.0812	0.1872
6	2.0	150	45/1.0	2.11	220/2.0	13.13	1.1400	0.2620
7	2.0	125	46/1.0	2.00	155/3.0	13.42	1.1420	0.2690
8	2.0	125	45/1.0	2.01	200/3.0	13.44	1.2100	0.2730
9	2.0	125	45/1.0	2.00	350/3.0	13.56	1.1500	0.2610

M = Concentration of Molar solution.

With the increase amount of raw PMS, the amount of product materials was found to be gradually increased (Table S1), which are illustrated in Fig. 1.

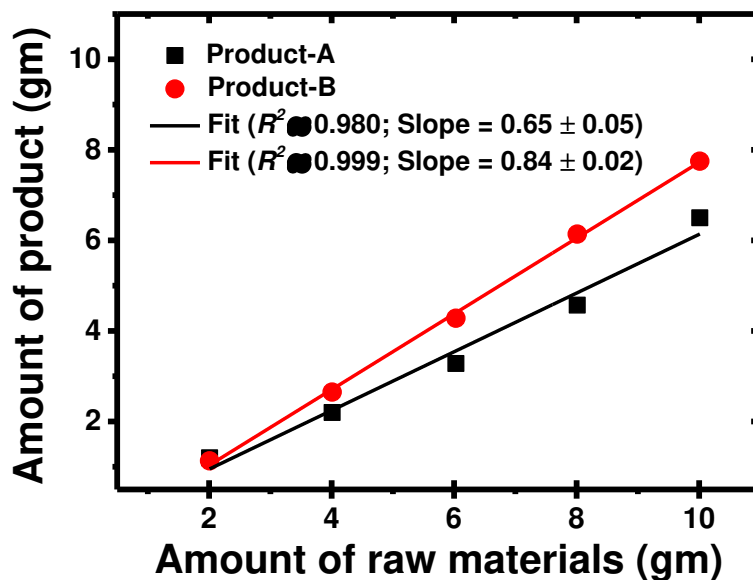


Figure 1: A correlation plot of the quantity of raw materials taken versus the amount of obtained product-A and product-B from different sampling batches.

According to this Fig. 1 it can be anticipated that the higher amount of starting sludge will provide the expected amount of calcium and this process is expected to be viable the industrial production. The average percentage of yield is about 65%, out of 2 g sample. The product obtained from a sample (a) and sample (b) is denoted as the product-A and product-B respectively. From Fig.1, it can also be inferred that Ca-compounds yield in product-B (slope = 0.84 ± 0.02) is higher compared to product-A (slope = 0.65 ± 0.05).

Owing to using waste material for the extraction of $\text{Ca}(\text{OH})_2$, it is very important to pre-investigate the raw sludge for identifying its chemical constituents, therefore, mineralogical study by means of X-ray fluorescence were performed. The obtained results are in oxide form and illustrated in Table 2 where CaO is in the highest amount: 95.9056 (wt.%) for source-A and 94.6093 (wt.%) for source-B of raw PMS materials.

Table 2: Wavelength Dispersive X-ray fluorescence (WDXRF) characterization of PMS sample source-A and sample source-B.

Components	Source-A/ wt.%	Source-B/ wt.%
Na ₂ O	0.0955	0.0299
MgO	0.2808	0.2916
Al ₂ O ₃	0.7067	0.4357
SiO ₂	1.1749	1.6297
P ₂ O ₃	0.0224	0.0190
SO ₃	0.0783	0.0506
NaCl	0.0968	0.0592
K ₂ O	0.0317	0.0395
CaO	95.9056	94.6093
Cr ₂ O ₃	0.2999	0.6586
MnO	-	0.1226
Fe ₂ O ₃	1.1674	1.9348
ZnO	0.0201	0.0388
Rb ₂ O	-	0.0083
SrO	0.0281	0.0355
ZrO ₂	0.0740	0.0249
Nb ₂ O	-	0.0120
TiO ₂	0.0178	-
Total	100.0000	100.0000

Apart from major mineral (Ca), other minerals were also found in trace level, except SiO₂ and Fe₂O₃ which were combinedly ~2.4%. This huge amount of calcium content in PMS motivated us to find a facile extraction process of calcium-hydroxide which was discussed in the materials and method section above. The extracted products were then systematically characterized by various characteristic tools and discussed below.

3.2. Surface morphology and chemical composition of the isolated product

The morphological features of the obtained product-A and product-B were explored by means of Scanning Electron Microscopy (SEM) and SEM micrographs are shown in Fig. 2.

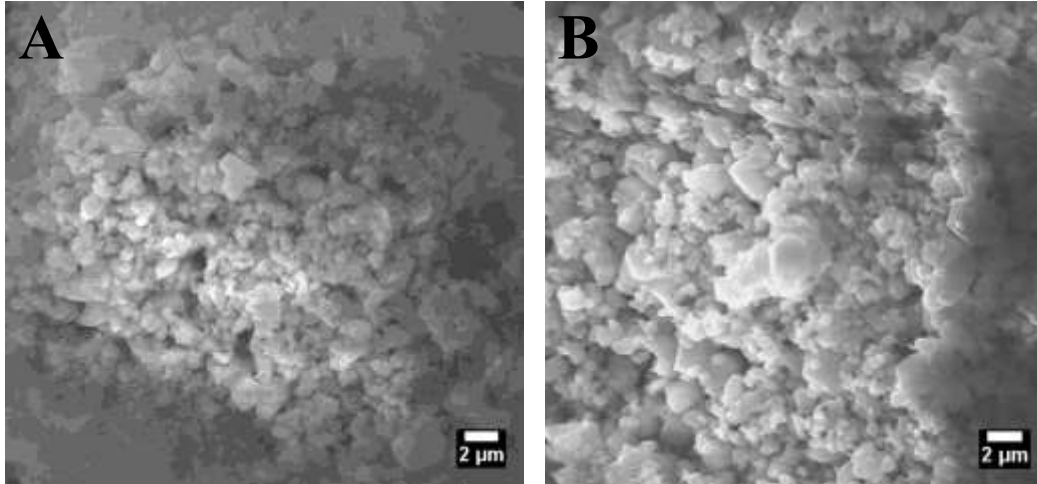


Figure 2: Surface morphology of isolated product-A (left) and product-B (right).

The SEM micrographs exhibit that the powder grains/particles in the synthesized products are polygons but with no uniform shape. The average particle size was determined by ImageJ software and it was found to be in the range of 450 – 500 nm for both products. Numerous studies in literature revealed the formation of Nano-calcium hydroxide with approximately similar morphologies and size [27, 28]. The elemental composition of product-A and product-B were also investigated by SEM/EDX microanalyzer and shown in Fig. 3.

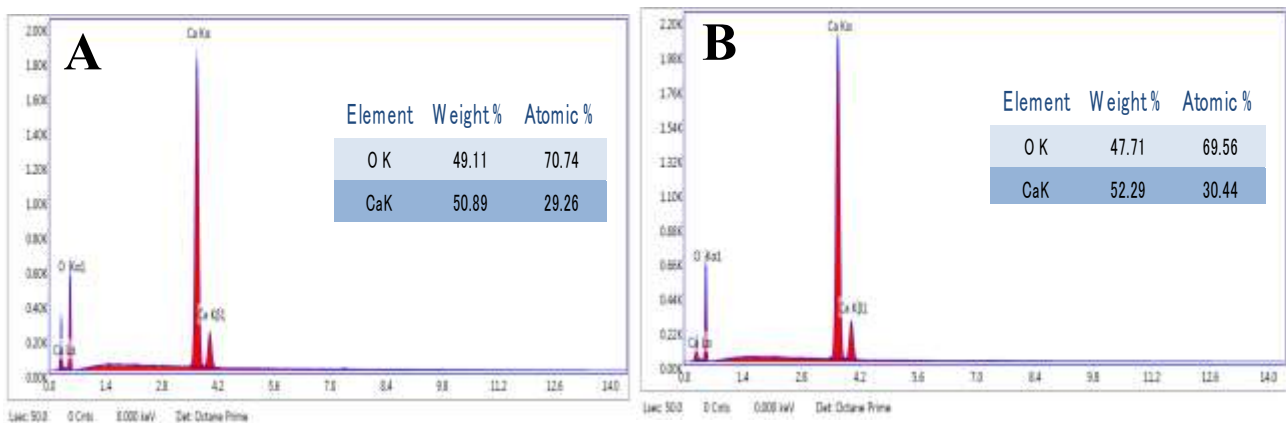


Figure 3: EDX microanalysis of synthesized product-A (left) and product-B (right). Their elemental compositions are shown in the inset tables.

In product-A and product-B, calcium content is 50.89% and 52.29% respectively and oxygen content is 49.11% and 47.71% respectively. These values (weight %) are summarized in two tables inside the respective figure (cf. Fig. 3). From the EDX microanalyses, it is evident that calcium-based compounds in product-B is slightly greater than that of the product-A corroborating the results shown in Fig. 1 above.

3.3. FTIR analyses

Figure 4 depicts FTIR patterns of the obtained product-A and product-B, where both spectra are approximately similar but with a little difference regarding the peak intensities. The reference FTIR curves of calcium-based compounds from RRUFF database [36] can be found in Figure S2.

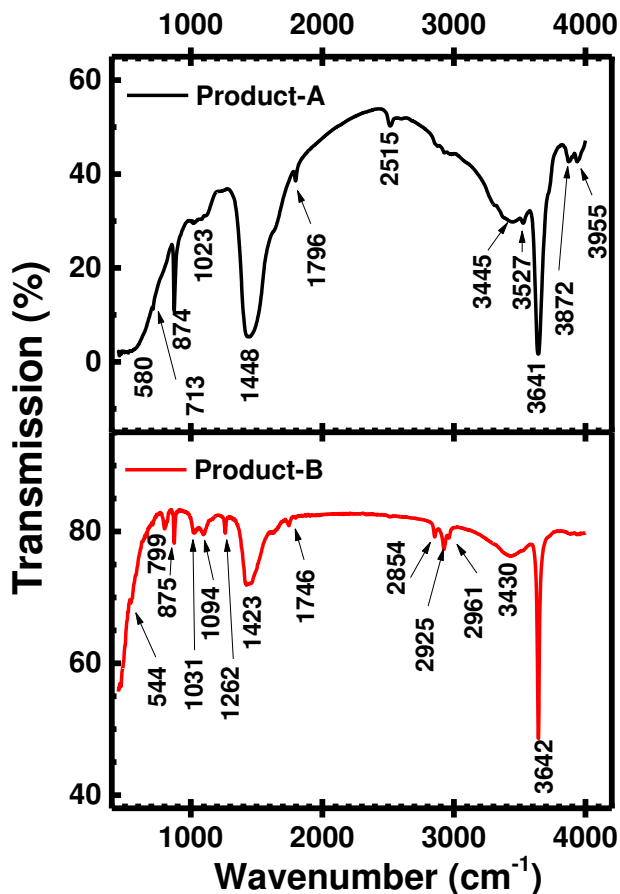


Figure 4: FTIR spectra of the isolated product-A and product-B from two different PMS sources.

The relatively strong absorption band at $\sim 3641\text{ cm}^{-1}$ (product-A) and $\sim 3642\text{ cm}^{-1}$ (product-B) corresponds to the stretching mode of hydroxyl group (OH) [1, 23, 37] (also see [Figure S2](#)). In addition, there has the possibility of some water molecules incorporation on the sample-surface from the air during sample handling [38]. The (OH) stretching band is noticeably sharp and may signify the pure calcium hydroxide phase [23]. The broadband peaks ranging from $\sim 3430\text{ cm}^{-1}$ to $\sim 3527\text{ cm}^{-1}$ also reveals the existence of corresponding OH stretching modes. Some common peaks, clustered from $\sim 2515\text{ cm}^{-1}$ to $\sim 2961\text{ cm}^{-1}$ and from $\sim 1746\text{ cm}^{-1}$ to $\sim 1796\text{ cm}^{-1}$, have been attributed to the adsorption of atmospheric CO_2 and stretching mode of C=O bond, respectively [23]. The broad stretching absorption and sharp peaks at $\sim 713\text{ cm}^{-1}$ and $\sim 799\text{ cm}^{-1}$, $\sim 874\text{ cm}^{-1}$ and $\sim 875\text{ cm}^{-1}$, and $\sim 1448\text{ cm}^{-1}$ and $\sim 1423\text{ cm}^{-1}$ (cf. product-A and product-B) represents ν_4 (in-plane-bending mode/ bending vibration), ν_2 (out-of-plane bending mode/ symmetric deformation), and ν_3 (anti-symmetric stretching mode) of carbonate group (CO_3^{2-}) of the calcite [1, 33, 39]. The peak value ranging from $\sim 1023\text{ cm}^{-1}$ to $\sim 1094\text{ cm}^{-1}$ is because of ν_1 (symmetric stretching mode) for the CO_3^{2-} group in calcite [23, 31]. In [Fig. 4](#) (product-B), peak value at $\sim 1262\text{ cm}^{-1}$ corresponds to the stretching mode of C-O bond in the CO_3^{2-} -group [40]. The wide and strong band peaks at $\sim 580\text{ cm}^{-1}$ and $\sim 544\text{ cm}^{-1}$ in [Fig. 2](#) illustrate the presence of Ca-O band of symmetric vibration [33, 39]. Additionally, the vibrational peaks at 3872 cm^{-1} and 3955 cm^{-1} in product-A indicate the vibrational mode of O-H [41]. In summary, FTIR analyses suggest that both Ca(OH)_2 and CaCO_3 are present in the synthesized products [23, 24].

3.4. XRD Analyses of PMS source and products

The XRD patterns of representative PMS source and synthesized products are illustrated in [Fig. 5](#) and the (hkl) reflections peaks are matched with the diffraction peaks of the portlandite (hexagonal Ca(OH)_2 , marked by *); calcite (rhombohedral CaCO_3 , marked by \square); and aragonite (orthorhombic CaCO_3 , marked by #) collected from the RRUFF database [36]. The XRD patterns of these calcium-based compounds can be found in [Figure S3](#) in the supplementary materials.

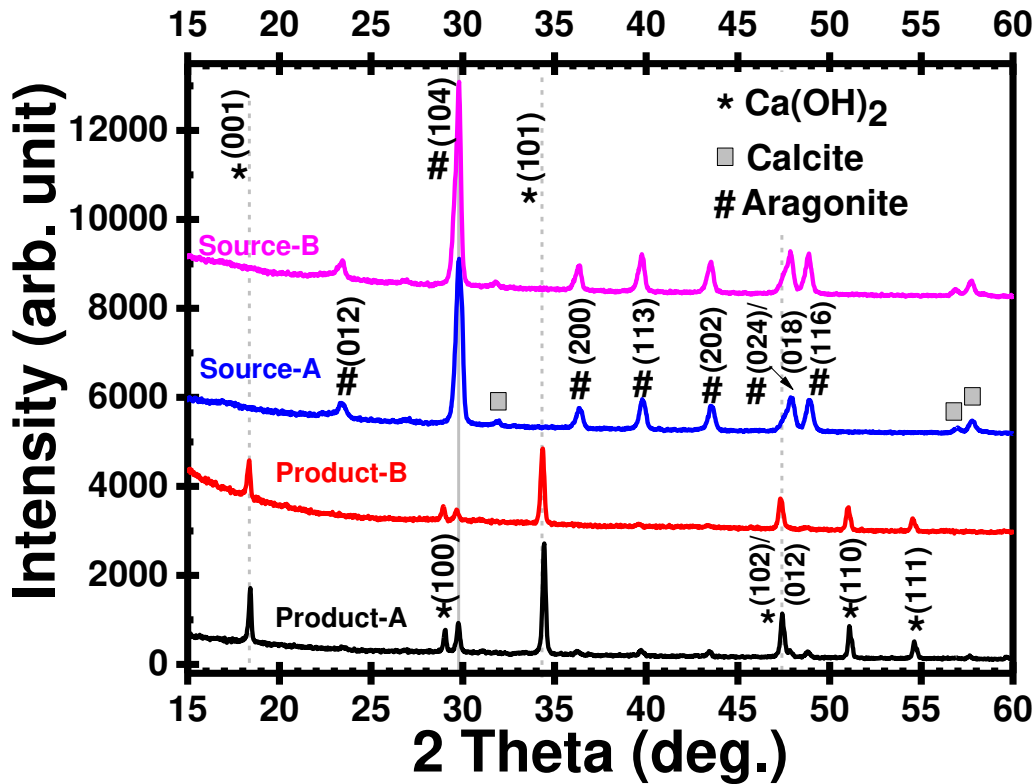


Figure 5: (vertically offset for clarity) XRD patterns of isolated product-A, product-B, source-A and source-B. Aragonite (#) and Calcite (□) are the two polymorphs of CaCO₃.

From Fig. 5, it is clear that PMS samples collected from source-A and source-B mainly composed of aragonite phase of CaCO₃ with small amount of calcite phase of CaCO₃ evident from the minor Bragg' peaks (marked by □) in the range of $2\theta = 30^\circ - 60^\circ$. No XRD peaks related to Ca(OH)₂ is detected. (Full scanning range ($2\theta = 10^\circ - 80^\circ$) XRD patterns of all samples can be found in Figure S4). In contrast, XRD patterns of both product-A and product-B exhibits diffraction peaks (marked by *) correspond to the hexagonal phase of Ca(OH)₂ having space group P-3m1 (Space Group No. 164, PDF Card No. 00-087-0673) [1, 23, 31]. For product A/B, these diffraction peaks are appeared at $2\theta = 18.42^\circ / 18.34^\circ$, $29.04^\circ / 28.94^\circ$, $34.44^\circ / 34.36^\circ$, $47.44^\circ / 47.32^\circ$, $51.10^\circ / 51.04^\circ$, $54.62^\circ / 54.52^\circ$, $62.88^\circ / 62.76^\circ$, $64.52^\circ / 64.42^\circ$, and $72.00^\circ / 71.88^\circ$ corresponded to the (001), (100), (101), (102), (110), (111), (021), (013), and (002) planes of the Ca(OH)₂. In addition, a minor Bragg' peak is appeared at $2\theta \sim 29.8^\circ$ which can be attributed to the #(104) plane of the orthorhombic CaCO₃ phase (denoted by solid line). Numerous studies in literature ([1, 23, 24, 31] and refs. therein) reported that the inevitable generic presence of Ca(OH)₂ and CaCO₃ phase is due

to the reaction of atmospheric CO₂ with Ca(OH)₂ (*aka* carbonation process) irrespective of the synthesis routes. However, in our study, taking the ratio of area under curves [42] of peak *(101) and #(104) suggest that Ca(OH)₂ content in product-B is 1.84 times higher compared to that of the product-A [Table S2]. These observations again suggest that synthesized products from PMS source are mainly composed of Ca(OH)₂ phase with small amount of CaCO₃ phase. This is consistent with the results presented in Fig.1, and Fig. 4.

In order to elucidate the mean crystallite domain size (*d*) of the synthesized product, the Scherrer's equation (1) [43] was utilized.

$$d = \frac{K\lambda}{\beta \cos\theta} \dots\dots\dots (1)$$

Where *K* is Scherer's constant, equal to 0.94, λ is the wavelength of X-ray radiation used ($\lambda = 1.5406 \text{ \AA}$), θ is the Bragg diffraction angle, and β is the full width at half maximum (FWHM) in radiation. The most prominent *(101) peak of Ca(OH)₂ was considered to estimate the mean crystal domain sizes and was found to be 41.96 nm (for product-A) and 36.49 nm (for product-B). While considering #(104) peak of CaCO₃, mean crystallite domain size was found to be 39.20 nm (for product-A) and 32.15 nm (for product-B) [cf. Figure S5 and Table S2]. It can be seen that diffraction peaks for product-A is slightly shifted to higher 2 θ values compared to that of the product-B (indicated by the major diffraction peaks of Ca(OH)₂ denoted by dashed line in Fig. 6) which presumably due to the stress-strain effect owing to the combined presence of Ca(OH)₂ and CaCO₃. The lattice strain, ϵ of crystal at the plane *(101) and #(104) were determined using the following expression (2) [43].

$$\epsilon = \frac{\beta}{4 \tan\theta} \dots\dots\dots (2)$$

The calculated value of the lattice strain was found to be 2.92×10^{-3} (product-A) and 3.36×10^{-3} (product-B) considering the plane *(101) of Ca(OH)₂ and 2.60×10^{-3} (product-A) and 4.40×10^{-3} (product-B) while considering the plane #(104) of CaCO₃. In both cases, microstrain in product-B is higher than that of product-A. To elucidate the origin of minor presence of CaCO₃ phase in the Ca(OH)₂ compound and therefore, their stress/strain-related effect, we have performed the Raman spectroscopic analyses systematically and discussed in the section 3.5 below.

3.5. Raman spectroscopic Analysis

Raman spectra of the isolated product-A, product-B, pure CaCO_3 and pure Ca(OH)_2 samples were recorded at room temperature and maintaining the same experimental conditions (i.e., same laser exposure time: 5 s, no. of accumulations: 5, laser power < 5 mW, spot size < dia. ~ 0.5 mm) and these spectra are shown in Fig. 6. The Ca(OH)_2 samples were left in open laboratory air for various time of durations and then Raman spectra were recorded after 30 min, 5 h, 24 h (1 day), 48 h (2 day), 144 h (6 day) duration for monitoring the CaCO_3 formation kinetics within the Ca(OH)_2 materials (see Fig. 6b).

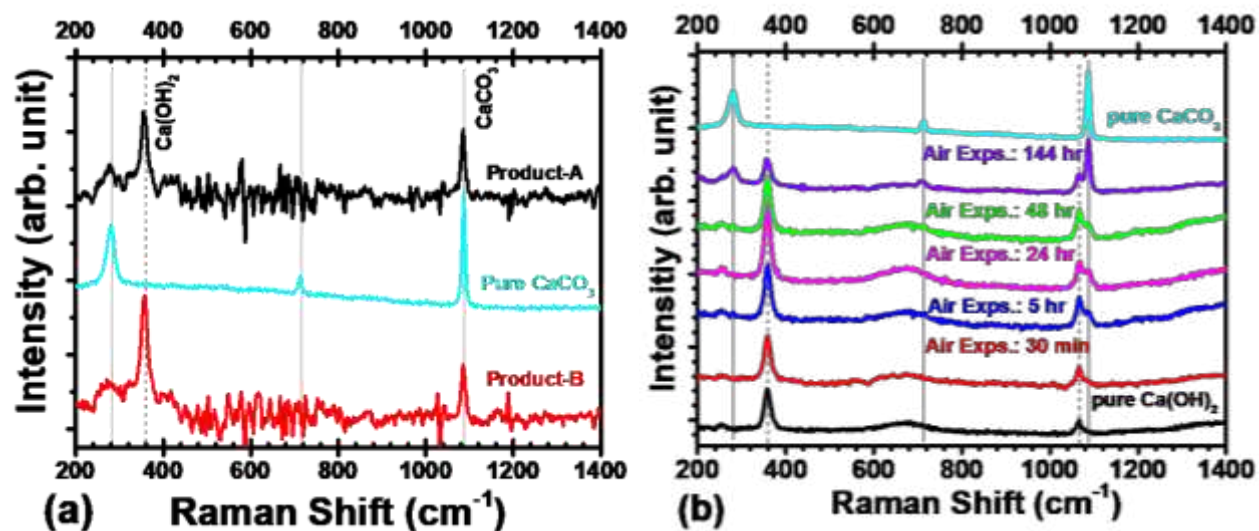


Figure 6: Room temperature Raman spectra of (a) the obtained product-A, product-B, and a reference CaCO_3 (purity $\sim 99.95\%$) sample; (b) pure Ca(OH)_2 (purity $\sim 99.95\%$) and the same Ca(OH)_2 with various air exposure duration (30 min, 5 hr, 24 hr, 48 hr and 144 hr). The solid and dashed vertical lines indicate the reference Raman peaks of CaCO_3 and Ca(OH)_2 respectively.

The Raman spectrum of the pure CaCO_3 samples exhibited vibrational peaks (solid lines) approximately at 157.18 cm^{-1} , 280.95 cm^{-1} , 713.46 cm^{-1} , and 1087.53 cm^{-1} and pure Ca(OH)_2 samples exhibited vibrational peaks (dashed lines) approximately at 359.72 cm^{-1} (357.66 cm^{-1} for 144 h air exposed Ca(OH)_2 sample), 1066.78 cm^{-1} which are very much consistent with their respective Raman spectrum from RUFF database (cf. Fig. 6 and Figure S2b). As can be seen from Fig. 6a, the Raman peaks at 353.53 cm^{-1} and 1085.65 cm^{-1} are seen for product-A while at 357.66 cm^{-1} and 1085.65 cm^{-1} are seen for product-B. These peak positions can be attributed to the Raman

peak value of Ca(OH)_2 ($\sim 360 \text{ cm}^{-1}$) and CaCO_3 ($\sim 1088 \text{ cm}^{-1}$) respectively. Notice also that peak size of Ca(OH)_2 in product-B is larger than that of product-A, suggesting a higher amount of calcium hydroxide in product-B compared to that of product-A corroborating the results shown in Fig. 1, Fig. 3, Fig. 5. Additionally, the Ca(OH)_2 peak in product-A is $\sim 4 \text{ cm}^{-1}$ red-shifted compared to that of product-B. This indicates the higher microstrain induced in product-B compared to product-A corroborating the XRD results (see Figure S6). This is presumably due to the higher amount of CaCO_3 inclusion in the product-B compared to product-A. Referring to the XRD analyses, we observed that Ca(OH)_2 Bragg's peaks in the both group of products is significantly higher than that of CaCO_3 (see Fig. 5). Numerous studies reported that the inclusion of CaCO_3 in air-exposed Ca(OH)_2 is inevitable due to the interaction of atmospheric CO_2 with Ca(OH)_2 [44, 45]. In Fig. Fig. 6b, we verified this inevitable carbonation process by analyzing Raman spectra of a pure Ca(OH)_2 sample which were systematically exposed in air for various durations. Notice that with the increase of air-exposure durations, the Ca(OH)_2 peak at $\sim 1066.78 \text{ cm}^{-1}$ (dashed line) is consistently decreasing with the increasing of the CaCO_3 peak (solid line) at $\sim 1087.53 \text{ cm}^{-1}$. With increasing CaCO_3 peak in the Ca(OH)_2 sample, major Raman peak of Ca(OH)_2 at $\sim 360 \text{ cm}^{-1}$ is slightly red-shifted compared to the pure sample (see Figure S3 in the supplemental materials for details). In summary, from all experimental results shown above, we can confirm that our extraction process yielded Ca(OH)_2 phase as major product from the two different PMS sources and minor inclusion of CaCO_3 phase in the products is due to their air-exposure in the laboratory which could be avoided by performing the extraction process either in the air-tight chamber or in the inert atmosphere.

4. Conclusion

This study demonstrates a facile extraction process of calcium hydroxide materials from paper mills sludge collected from two different sources. To the best of our knowledge, we have utilized paper mill's waste of Bangladesh for the first time to extract this valuable chemical. In addition, it is accomplished in the water at room temperature by a common, without ionic & non-ionic surfactant, low energy-intensive and cost-effective chemical precipitation method. Due to the well-known carbonation process, a small presence of CaCO_3 phase was detected by FTIR, Raman, and XRD. However, all the presented results conducted by a variety of characterizations tools

conspicuously reveals that synthesis products from the both PMS source are mainly composed of calcium hydroxide. Only acid and base treatment with a certain range of P^H in the two different medium gives our method a great potential to implement in the recycling sectors of pulp and paper industries for the extraction of valuable calcium-based compounds as well as recycling the waste sludge.

Author Contributions:

Credit Authorship contribution statement

Mohammad Robel Molla: Investigation, Validation, Formal analysis, Methodology, Writing - original draft. **Most. Hosney Ara Begum:** Conceptualization, Investigation, Validation, Methodology, Formal analysis, Project administration, Supervision, Writing - original draft. **Syed Farid Uddin Farhad:** Conceptualization, Formal analysis, Writing - review & editing and lead the project works towards publications. **A.S.M. Asadur Rahman:** Investigation, Validation. **Nazmul Islam Tanvir:** Investigation, Methodology, Visualization. **Muhammad Shahriar Bashar:** Investigation. **Riyadh Hossen Bhuiyan:** Investigation. **Md. Sha Alam:** Investigation. **Mohammad Sajjad Hossain:** Investigation, Visualization. **Mir Tamzid Rahman:** Conceptualization, Validation, Methodology, Formal analysis, Supervision.

Declaration of Competing Interest:

The authors have declared that no competing interest exists.

Acknowledgement:

All authors are thankful to the authority of BCSIR for all kind of supports and encouragement to carry out this research work. The contributions of Suravi Islam, Principal scientific officer, IPD, BCSIR Laboratories, Dhaka and Nazia Khatun, Senior scientific officer, IPD, BCSIR Laboratories, Dhaka as part of the institutional infrastructural supports is greatly acknowledged by all authors.

References:

- [1] H. Vu, M. Khan, R. Chilakala, T. Lai, T. Thenepalli, J. Ahn, *et al.*, "Utilization of Lime Mud Waste from Paper Mills for Efficient Phosphorus Removal," *Sustainability*, vol. 11, p. 1524, 2019.
- [2] J. He, C. R. Lange, and M. Dougherty, "Laboratory study using paper mill lime mud for agronomic benefit," *Process Safety and Environmental Protection*, vol. 87, pp. 401-405, 2009/11/01/ 2009.
- [3] H. Nurmesniemi, R. Pöykö, and R. L. Keiski, "A case study of waste management at the Northern Finnish pulp and paper mill complex of Stora Enso Veitsiluoto Mills," *Waste Management*, vol. 27, pp. 1939-1948, 2007/01/01/ 2007.
- [4] Y. Zhou, H. Zhao, H. Bai, L. Zhang, and H. Tang, "Papermaking Effluent Treatment: A New Cellulose Nanocrystalline/Polysulfone Composite Membrane," *Procedia Environmental Sciences*, vol. 16, pp. 145-151, 2012/01/01/ 2012.
- [5] I. Tiseo. (2021, 27/08/2021). *Global paper industry -statistics and facts*. Available: <https://www.statista.com/topics/1701/paper-industry/>
- [6] I. Tiseo. (2021, 27/08/2021). *Production volume of paper and cardboard in major countries from 2009 to 2018*. Available: <https://www.statista.com/statistics/240598/production-of-paper-and-cardboard-in-selected-countries/>
- [7] I. Natali, P. Tempesti, E. Carretti, M. Potenza, S. Sansoni, P. Baglioni, *et al.*, "Aragonite Crystals Grown on Bones by Reaction of CO₂ with Nanostructured Ca(OH)₂ in the Presence of Collagen. Implications in Archaeology and Paleontology," *Langmuir*, vol. 30, pp. 660-668, 2014/01/21 2014.
- [8] R. Giorgi, D. Chelazzi, and P. Baglioni, "Nanoparticles of Calcium Hydroxide for Wood Conservation. The Deacidification of the Vasa Warship," *Langmuir*, vol. 21, pp. 10743-10748, 2005/11/01 2005.
- [9] L. Dei and B. Salvadori, "Nanotechnology in cultural heritage conservation: nanometric slaked lime saves architectonic and artistic surfaces from decay," *Journal of Cultural Heritage*, vol. 7, pp. 110-115, 2006/04/01/ 2006.
- [10] M. Sadeghi and M. H. Hussein, "A Novel Method for the Synthesis of CaO Nanoparticle for the Decomposition of Sulfurous Pollutant," *Journal of Applied Chemical Research*, vol. 7, pp. 39-49, 2013.
- [11] A. Islam, S. H. Teo, E. S. Chan, and Y. H. Taufiq-Yap, "Enhancing the sorption performance of surfactant-assisted CaO nanoparticles," *RSC Advances*, vol. 4, pp. 65127-65136, 2014.
- [12] R. L. Berger, D. S. Cahn, and J. D. McGregor, "Calcium Hydroxide as a Binder in Portland Cement Paste," *Journal of the American Ceramic Society*, vol. 53, pp. 57-58, 1970/01/01 1970.
- [13] B. D. Barnes, S. Diamond, and W. L. Dolch, "Micromorphology of the Interfacial Zone Around Aggregates in Portland Cement Mortar," *Journal of the American Ceramic Society*, vol. 62, pp. 21-24, 1979/01/01 1979.
- [14] S. K. Swain, S. Bhattacharyya, and D. Sarkar, "Fabrication of porous hydroxyapatite scaffold via polyethylene glycol-polyvinyl alcohol hydrogel state," *Materials Research Bulletin*, vol. 64, pp. 257-261, 2015/04/01/ 2015.
- [15] G. Jaria, V. Calisto, C. P. Silva, M. V. Gil, M. Otero, and V. I. Esteves, "Obtaining granular activated carbon from paper mill sludge – A challenge for application in the removal of pharmaceuticals from wastewater," *Science of The Total Environment*, vol. 653, pp. 393-400, 2019/02/25/ 2019.
- [16] A. Farhad and Z. Mohammadi, "Calcium hydroxide: a review," *International Dental Journal*, vol. 55, pp. 293-301, 2005/10/01/ 2005.
- [17] M. El Bakkari, V. Bindiganavile, and Y. Boluk, "Facile Synthesis of Calcium Hydroxide Nanoparticles onto TEMPO-Oxidized Cellulose Nanofibers for Heritage Conservation," *ACS Omega*, vol. 4, pp. 20606-20611, 2019/12/10 2019.

- [18] N. A. Oladoja, I. A. Ololade, S. E. Olaseni, V. O. Olatujoye, O. S. Jegede, and A. O. Agunloye, "Synthesis of Nano Calcium Oxide from a Gastropod Shell and the Performance Evaluation for Cr (VI) Removal from Aqua System," *Industrial & Engineering Chemistry Research*, vol. 51, pp. 639-648, 2012/01/18 2012.
- [19] A. Nanni and L. Dei, "Ca(OH)₂ Nanoparticles from W/O Microemulsions," *Langmuir*, vol. 19, pp. 933-938, 2003/02/01 2003.
- [20] M. Amin Alavi and A. Morsali, "Ultrasonic-assisted synthesis of Ca(OH)₂ and CaO nanostructures," *Journal of Experimental Nanoscience*, vol. 5, pp. 93-105, 2010/04/01 2010.
- [21] T. Liu, Y. Zhu, X. Zhang, T. Zhang, T. Zhang, and X. Li, "Synthesis and characterization of calcium hydroxide nanoparticles by hydrogen plasma-metal reaction method," *Materials Letters*, vol. 64, pp. 2575-2577, 2010/12/15/ 2010.
- [22] G. Taglieri, C. Mondelli, V. Daniele, E. Pusceddu, and A. Trapananti, "Synthesis and X-Ray Diffraction Analyses of Calcium Hydroxide Nanoparticles in Aqueous Suspension," *Advances in Materials Physics and Chemistry*, vol. Vol.03No.01, p. 5, 2013.
- [23] A. Samanta, D. K. Chanda, P. S. Das, J. Ghosh, A. K. Mukhopadhyay, and A. Dey, "Synthesis of Nano Calcium Hydroxide in Aqueous Medium," *Journal of the American Ceramic Society*, vol. 99, pp. 787-795, 2016/03/01 2016.
- [24] C. Rodriguez-Navarro, A. Suzuki, and E. Ruiz-Agudo, "Alcohol Dispersions of Calcium Hydroxide Nanoparticles for Stone Conservation," *Langmuir*, vol. 29, pp. 11457-11470, 2013/09/10 2013.
- [25] G. Taglieri, C. Mondelli, V. Daniele, E. Pusceddu, and G. Scoccia, "Synthesis, Textural and Structural Properties of Calcium Hydroxide Nanoparticles in Hydro-Alcoholic Suspension," *Advances in Materials Physics and Chemistry*, vol. Vol.04No.03, p. 10, 2014.
- [26] V. Daniele and G. Taglieri, "Nanolime suspensions applied on natural lithotypes: The influence of concentration and residual water content on carbonation process and on treatment effectiveness," *Journal of Cultural Heritage*, vol. 11, pp. 102-106, 2010/01/01/ 2010.
- [27] B. Salvadori and L. Dei, "Synthesis of Ca(OH)₂ Nanoparticles from Diols," *Langmuir*, vol. 17, pp. 2371-2374, 2001/04/01 2001.
- [28] E. Carretti, D. Chelazzi, G. Rocchigiani, P. Baglioni, G. Poggi, and L. Dei, "Interactions between Nanostructured Calcium Hydroxide and Acrylate Copolymers: Implications in Cultural Heritage Conservation," *Langmuir*, vol. 29, pp. 9881-9890, 2013/08/06 2013.
- [29] V. Daniele and G. Taglieri, "Synthesis of Ca(OH)₂ nanoparticles with the addition of Triton X-100. Protective treatments on natural stones: Preliminary results," *Journal of Cultural Heritage*, vol. 13, pp. 40-46, 2012/01/01/ 2012.
- [30] S. Zhang, "A new nano-sized calcium hydroxide photocatalytic material for the photodegradation of organic dyes," *RSC Advances*, vol. 4, pp. 15835-15840, 2014.
- [31] A. Samanta, D. K. Chanda, P. S. Das, J. Ghosh, A. Dey, S. Das, *et al.*, "Synthesis of mixed calcite-calcium oxide nanojasmine flowers," *Ceramics International*, vol. 42, pp. 2339-2348, 2016/02/01/ 2016.
- [32] A. Anantharaman, S. Ramalakshmi, and M. George, "Green synthesis of calcium oxide nanoparticles and its applications," *Int. J. Eng. Res. Appl*, vol. 6, pp. 27-31, 2016.
- [33] W. Siriprom, K. Teanchai, K. Kirdsiri, and J. Kaewkhao, "Characterization of Calcium Hydroxide Derived from Waste Eggshell upon Moisture Effect," *Advanced Materials Research*, vol. 979, pp. 435-439, 2014.
- [34] N. Asikin-Mijan, Y. H. Taufiq-Yap, and H. V. Lee, "Synthesis of clamshell derived Ca(OH)₂ nanoparticles via simple surfactant-hydration treatment," *Chemical Engineering Journal*, vol. 262, pp. 1043-1051, 2015/02/15/ 2015.
- [35] A. Roy and J. Bhattacharya. (2010, Synthesis of Ca(OH)₂ nanoparticles by wet chemical method. *Micro & Nano Letters* 5(2), 131-134. Available: <https://digital-library.theiet.org/content/journals/10.1049/mnl.2010.0020>

- [36] B. Downs and H. Yang. Integrated database of Raman spectra, X-ray diffraction and chemistry data for minerals [Online]. Available: <https://rruff.info/>
- [37] P. Lagarde, M. A. H. Nerenberg, and Y. Farge, "Ca(OH)₂ Infrared Vibrational Spectra around 3600 cm⁻¹ : Experimental and Theoretical Study on Microcrystals and Single Crystals," *Physical Review B*, vol. 8, pp. 1731-1746, 08/15/ 1973.
- [38] M. Ghiasi and A. Malekzadeh, "Synthesis of CaCO₃ nanoparticles via citrate method and sequential preparation of CaO and Ca(OH)₂ nanoparticles," *Crystal Research and Technology*, vol. 47, pp. 471-478, 2012/04/01 2012.
- [39] T. Witton, "Characterization of calcium oxide derived from waste eggshell and its application as CO₂ sorbent," *Ceramics International*, vol. 37, pp. 3291-3298, 2011/12/01/ 2011.
- [40] B. Stuart, W. O. George, and P. S. McIntyre, *Modern Inferred Spectroscopy*. University of Greenwich, UK, 1998.
- [41] M. Galvan-Ruiz, L. Banos, and M. E. Rodriguez-Garcia, "Lime characterization as a food additive," *Sensing and Instrumentation for Food Quality and Safety*, vol. 1, pp. 169-175, 2007.
- [42] S. F. U. Farhad, "The effect of substrate temperature and oxygen partial pressure on the properties of nanocrystalline copper oxide thin films grown by pulsed laser deposition," *Data in Brief*, vol. 34, p. 106644, 2021/02/01/ 2021.
- [43] B. C. Ghos, S. F. U. Farhad, M. A. M. Patwary, S. Majumder, M. A. Hossain, N. I. Tanvir, *et al.*, "Influence of the Substrate, Process Conditions, and Postannealing Temperature on the Properties of ZnO Thin Films Grown by the Successive Ionic Layer Adsorption and Reaction Method," *ACS Omega*, vol. 6, pp. 2665-2674, 2021/02/02 2021.
- [44] T. Schmid and P. Dariz, "Shedding light onto the spectra of lime: Raman and luminescence bands of CaO, Ca(OH)₂ and CaCO₃," *Journal of Raman Spectroscopy*, vol. 46, pp. 141-146, 2015.
- [45] M. Tlili, M. B. Amor, C. Gabrielli, S. Joiret, G. Maurin, and P. Rousseau, "Characterization of CaCO₃ hydrates by micro-Raman spectroscopy," *Journal of Raman spectroscopy*, vol. 33, pp. 10-16, 2002.

Supplementary Files

This is a list of supplementary files associated with this preprint. Click to download.

- [GraphicalAbstractRobel.jpg](#)
- [SupplementaryInfoofPMS13.08.2021.docx](#)